

Supporting information

Fast and Reversibly Switchable Wettability Induced by Photothermal Effect

Jinseok Byun, Jihyun Shin, Seungchul Kwon, Sangshin Jang and Jin Kon Kim*

National Creative Research Center for Block Copolymer Self-Assembly and Departments of Chemical Engineering, Pohang University of Science and Technology (POSTECH), San 31 Hyoja-dong, Pohang 790-784, Republic of Korea

S1. Experimental details

Preparation of the gold nanoparticles: Gold nanoparticles with a diameter of ~ 40 nm were prepared by the growth of the seeds of small gold nanoparticles with a diameter 3.5 ± 0.7 nm, as previously reported.¹ During the preparation of large gold nanoparticles, gold nanorods with a length of ~200 nm and a diameter of 17 nm were also formed (~ 10 vol %). These nanorods were separated by centrifugation. Finally, excess cetyltrimonium bromide (CTAB) not capped on the gold nanoparticle surfaces was completely removed by centrifugation at 8,000 rpm for 30 min. Fig S1 shows the UV-vis spectrum and TEM image (inset) of the gold nanoparticles. UV-visible spectrum of colloidal gold nanoparticle solution was acquired with a UV-visible spectrometer (Varian, Cary-5000) in wavelengths between 300 to 800 nm. The shape and size of gold nanoparticles were characterized by transmission electron microscope (TEM) (Hitachi-7600).

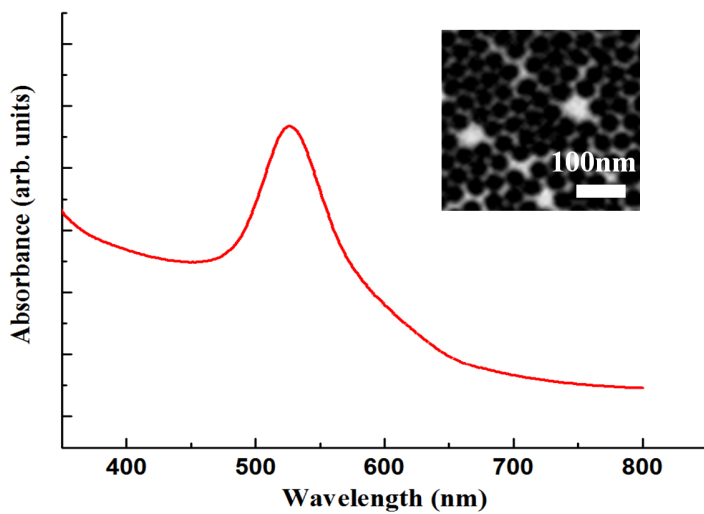


Fig S1. UV-vis spectrum (inset: TEM image) of gold nanoparticles with average diameter of ~ 40 nm.

Preparation of polyelectrolyte/nanoparticles multilayer film: The LBL technique by using electrostatic self-assembly was employed. Polyelectrolytes (PEI, PAH, PSS), silica and gold nanoparticles were used to prepare the nanoporous multilayer film. The roughness-enhanced (PEI)/(PSS/PAH)₅(SiO₂/PAH)₁₀

multilayer film on a silicon wafer was prepared as described in the previous report.² After being treated by piranha solution, the Si wafer was rinsed with DI-water and dried under nitrogen gas. The cleaned Si wafer was immersed in 40 mM PEI solution for 5 min and rinsed with DI-water three times. The sample was dried under nitrogen gas flow. The PEI-modified sample was alternately immersed in 40 mM PSS solution and 40 mM PAH solution (pH 7) for 5 min, and excessively washed by DI-water. Finally, the sample was dried on the hot plate for 1 min at each step. These processes were repeated five times. Then, the (PEI)/(PSS/PAH)₅ film was immersed in 0.05 wt% aqueous SiO₂ nanoparticle (Aldrich, d ~ 11 nm) solution and 40 mM PAH solution for 5 min alternately and excessively rinsed with DI water. The sample was then dried on the hot plate for 1 min. These processes were repeated ten times.

To fabricate (PSS/Au)₂₀ multilayer on PEI/(PSS/PAH)₅(SiO₂/PAH)₁₀ multilayer film, the sample was alternately immersed in a solution consisting of PSS and 2.5 M calcium chloride (CaCl₂, Aldrich, 98%) and aqueous solution of gold nanoparticles for 10 min and 30 min. After being excessively washed by DI-water, the sample was dried on the hot plate for 1 min at each step. These procedures were repeated twenty times. The roughness increased with increasing the deposition cycle.

Synthesis of PNIPAM chains grafted on gold nanoparticle by SI-ATRP: First, (SiO₂/PAH)₁₀(PSS/Au)₂₀ multilayer film containing gold nanoparticles was cleaned by using a UV-ozone light for 30 min. The sample was washed with ethanol and dried under a nitrogen flow. To graft the ATRP initiator, the cleaned sample was immersed in 0.1 M cysteamine (Aldrich, 95%) in ethanol for 2 h, resulting in the NH₂ terminated gold surface. The sample was washed with toluene and ethanol to remove unreacted cysteamine, and dried at 50 °C for 2h. The amine-modified substrate was immersed in 80 ml of dichloromethane containing pyridine (2 % w/v). 1 ml of 2-bromoisobutyryl bromide (Sigma-Aldrich, 98%), initiator of ATRP, was dropwise added at 0 °C under a continuous stream of nitrogen, the sample was left for 1h and at room temperature for 12h. The initiator grafted substrate was cleaned with acetone and toluene, and dried under the nitrogen flow.

The polymerization solution was prepared as follows.³ An organometallic catalyst solution was prepared by adding a 12.5 mg of Cu(I)Br (Sigma-Aldrich 98%, 0.085 mmol) to 5 mL solution of N, N, N', N', N"-pentamethyldiethyltriamine (PMDETA, 99% Acros Organics, 100μl, 0.48 mmol) in methanol. Finally, a 1.5 ml portion of catalyst solution was added to the NIPAM (99%, Acros Organics) monomer solution (8.4g, 74mmol) in 38 ml of DI water under the nitrogen gas flow.

After degassing, the polymerization solution was transferred into the initiator-grafted sample. PNIPAM was polymerized for 15 min at room temperature under a continuous stream of nitrogen, and the sample was rinsed with ethanol and DI water and dried under the flow of nitrogen gas.

Characterization: Field emission scanning electron microscope (FE-SEM) (Hitachi S-4800) was used to observe the top and cross-sectional morphology of the nanoporous multilayer. Atomic force microscope (AFM) (Nanoscope IIIa, Digital Instruments Multimode) in a tapping-mode was used to characterize the

surface roughness. The grafted PNIPAM chains were analyzed by using attenuated total reflectance Fourier transform infra-red spectroscope (ATR-FTIR) (BRUKER). Approximately 1000 scans were collected between 4000 and 1200 cm⁻¹ with a spectral resolution of 4 cm⁻¹. X-ray photoelectron spectroscopy (XPS) (ESCALAB 220 iXL (X-ray source: monochromated AlK α), VG Scientific) was also used to confirm the presence of PNIPAM on the surface.

An IR thermometer (Raytek, Raynger ST: temperature range from 32 to 535 °C with a resolution less than 0.1 °C) and thermal imaging camera were used to observe the surface temperature during the visible light illumination. The diode-pumped laser was used at a power density of 700 mW cm⁻² (WavescanTM, Coherent 899-01 R110 (532 nm)). The water contact angles were recorded at ambient temperature by using a droplet of 2 μ l. After all the images were acquired, precise digital analysis was performed to determine the contact angle.

S2. Analysis of the surface roughness

Fig S2 gives AFM images and surface profiles for (SiO₂/PAH)₁₀ and (SiO₂/PAH)₁₀(PSS/Au)₂₀ multilayer films. The root mean square roughness (R_{rms}) of the (SiO₂/PAH)₁₀ multilayer film was 62 ± 11 nm. Once the (PSS/Au)₂₀ was deposited on the (SiO₂/PAH)₁₀, the R_{rms} increases to 141 ± 5 nm. The roughness enhanced nanoporous multilayer was needed to obtain superhydrophobic surface.

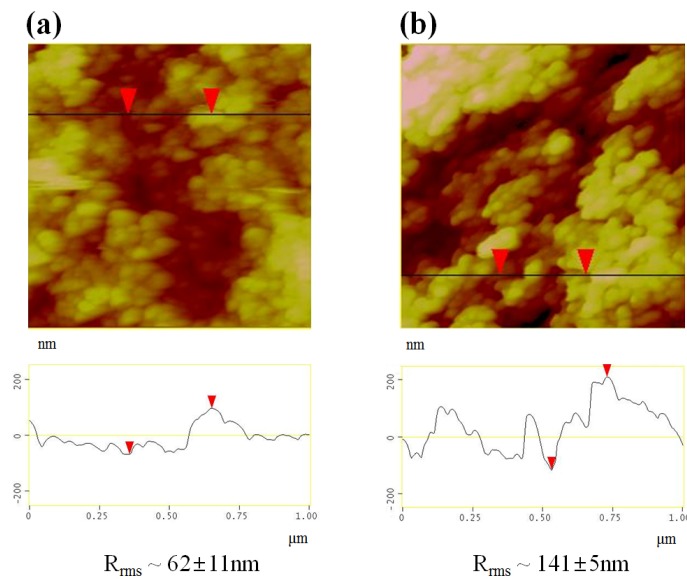


Fig S2. AFM images and surface profiles of (a) (SiO₂/PAH)₁₀ and (b) (SiO₂/PAH)₁₀(PSS/Au)₂₀ multilayer films.

S3. FT-IR and XPS measurements

Fig S3 shows the ATR-FTIR spectrum of the PNIPAM chains grafted on gold nanoparticles. The characteristic PNIPAM peaks were observed at 2970 cm^{-1} (antisymmetric stretching vibration of CH_3), 1640 cm^{-1} (C=O), 1370 cm^{-1} (the mixed vibration of C-N and N-H) and at 1450 cm^{-1} (antisymmetric deformation of CH_3). These peaks are essentially the same as pure PNIPAM.⁴ Therefore we concluded that PNIPAM was successfully synthesized by SI-ATRP.

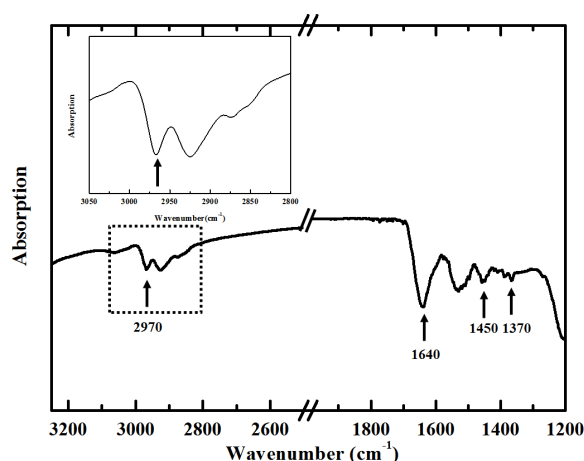


Fig S3. FT-IR spectrum of PNIPAM chains grafted on gold nanoparticles on the $(\text{SiO}_2/\text{PAH})_{10}(\text{PSS}/\text{Au})_{20}$ multilayer film.

The PNIPAM chains grafted on gold nanoparticles were also analyzed by XPS. Based on Fig S4, the ratio of nitrogen to carbon peak area in XPS spectrum is calculated to be 0.159, which is almost identical to that of pure PNIPAM. Also, we did not see any peak belonging to Au, indicating PNIPAM chains covered all of the gold nanoparticle surfaces.

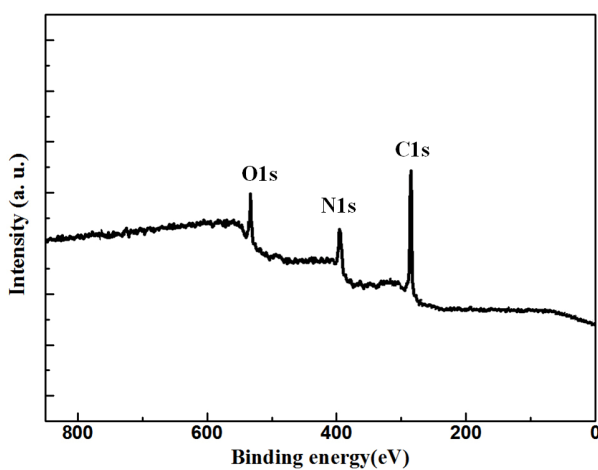


Fig S4. XPS spectra of PNIPAM covered multilayer film.

S4. Photothermal effect of $(\text{SiO}_2/\text{PAH})_{10}(\text{PSS}/\text{Au})_{20}$ multilayer film

To verify the photothermal effect of the gold nanoparticles, the multilayer film containing gold nanoparticles was irradiated by the diode-pumped laser at a power density of 700 mW cm^{-2} with a wavelength of 532 nm. Fig S5 gives the temperature change of the $(\text{SiO}_2/\text{PAH})_{10}$, $(\text{SiO}_2/\text{PAH})_{10}(\text{PSS}/\text{Au})_{10}$ and $(\text{SiO}_2/\text{PAH})_{10}(\text{PSS}/\text{Au})_{20}$ multilayer. The maximum surface temperature of the film after 15 min illumination for $(\text{SiO}_2/\text{PAH})_{10}$ multilayer film was only 2.4°C . Thus, the temperature increase by the laser itself without gold nanoparticles could be negligible. The maximum temperature increase for $(\text{SiO}_2/\text{PAH})_{10}(\text{PSS}/\text{Au})_{10}$ and $(\text{SiO}_2/\text{PAH})_{10}(\text{PSS}/\text{Au})_{20}$ multilayer films was 6.4°C and 15.0°C , respectively. Since the T_{LCST} of PNIPAM with water is 32°C , we need 20 layers of the gold nanoparticles for the surface temperature to be higher than the T_{LCST} after the laser irradiation.

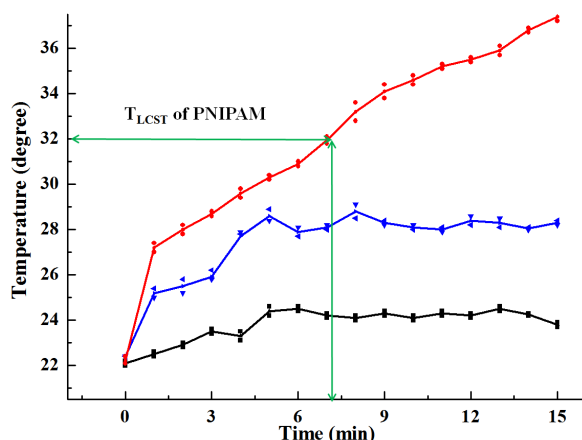


Fig S5. The change of the temperature of $(\text{SiO}_2/\text{PAH})_{10}$ (black), $(\text{SiO}_2/\text{PAH})_{10}(\text{PSS}/\text{Au})_{10}$ (blue), and $(\text{SiO}_2/\text{PAH})_{10}(\text{PSS}/\text{Au})_{20}$ (red) multilayer with the illumination time after turning on (and off) the laser with the power density of 700 mW cm^{-2} .

S5. Dynamic water contact angle and hysteresis

We also characterized the dynamic water CA of the superhydrophobic surface by measuring the advancing and receding CAs. The sliding behavior of water droplet on the surface with a tilting angle of 4° is shown in Fig S6. The advancing and receding contact angles were recorded while the water droplet spontaneously moved on the tilted surface. From Figure S6, the advancing CA (θ_A) and receding CA(θ_R) are $155.3 \pm 2.0^\circ$ and $151.1 \pm 1.7^\circ$, respectively. Water droplet rolled off on the tilted surface with very small hysteresis ($\sim 4^\circ$) in CA, indicating that the illuminated surface is indeed superhydrophobic.⁵

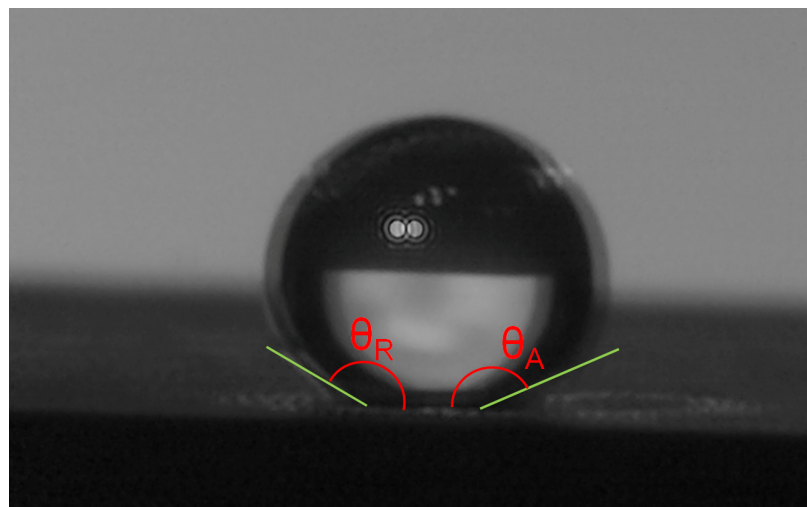


Fig S6. Photograph of a water droplet rolling off on the illuminated surface with a tilting angle of 4°.

References

- 1 N. R. Jana, L. Gearheart, C. J. Murphy, *Langmuir* 2001, **17**, 6782.
- 2 H. S. Lim, J. T. Han, D. Kwak, M. H. Jin, K. Cho, *J. Am. Chem. Soc.* 2006, **128**, 14458.
- 3 H. Gehan, L. Fillaud, M. M. Chehimi, J. Aubard, A. Hohenau, N. Felidj, C. Mangeney, *ACS Nano* 2010, **4**, 6491.
- 4 L. Liang, P. C. Rieke, J. Liu, G. E. Fryxell, J. S. Young, M. H. Engelhard, K. L. Alford, *Langmuir* 2000, **16**, 8016.
- 5 L. Liu, J. Zhao, Y. Zhang, F. Zhao, Y. Zhang, *J. Colloid Interface Sci.* 2011, **358**, 277.